

## Development of 600-MHz $^{19}\text{F}$ - $^7\text{Li}$ Solid-State NMR Probe for *In-Situ* Analysis of Lithium Ion Batteries

Ji-Ho Jeong, Yu-Geun Park, Sung-Sub Choi, and Yongae Kim\*

Department of Chemistry, Hankuk University of Foreign Studies, Yongin 449-791, Korea. \*E-mail: yakim@hufs.ac.kr  
Received June 2, 2013, Accepted August 7, 2013

Lithium is a highly attractive material for high-energy-concentration batteries, since it has low weight and high potential. Rechargeable lithium-ion batteries (LIBs), which have the extremely high gravimetric and volumetric energy densities, are currently the most preferable power sources for future electric vehicles and various portable electronic devices. In order to improve the efficiency and lifetime, new electrode compounds for lithium intercalation or insertion have been investigated for rechargeable batteries. Solid-state nuclear magnetic resonance (NMR) is a very useful tool to investigate the structural changes in electrode materials in actual working lithium-ion batteries. To detect the *in-situ* microstructural changes of electrode and electrolyte materials,  $^7\text{Li}$ - $^{19}\text{F}$  double-resonance solid-state NMR probe with a static solenoidal coil for a 600-MHz narrow-bore magnet was designed, constructed, and tested successfully.

**Key Words** :  $^7\text{Li}$ - $^{19}\text{F}$  double resonance, Solid-state NMR Probe, Lithium-Ion Battery (LIB), Electrode, Electrolyte

### Introduction

Energy storage plays an important role in industry. Since lithium has a low weight and high potential, it is a highly attractive material for high-energy-concentration batteries. So, lithium-ion batteries have been widely used for electric vehicles and various portable electronic devices. The remarkable recent developments in portable electronic applications have been the major driving force for studies of batteries with high energy density and flexible form. In order to improve the efficiency and lifetime, new electrode compounds for lithium intercalation or insertion have been investigated for rechargeable batteries.<sup>1-3</sup> Despite safety issues and the use of cobalt,  $\text{Li}(\text{Co},\text{Ni})\text{O}_2$  has been considered as an active cathode material in recent years because of its efficiency.<sup>4-6</sup> Recently, Padhi *et al.* suggested the possibility of using a novel compound,  $\text{LiFePO}_4$ , which has olivine structure, as the cathode for lithium batteries. This material is environmentally benign and inexpensive. Moreover, the structure of  $\text{LiFePO}_4$  remains unchanged at up to 400 °C, and the primary characteristic of the crystal structure is conserved, making the compounds stable during cycling with no temperature limitations. However, the practical capacity of 100-110  $\text{mAh}^{-1}\text{g}$  associated with  $\text{LiFePO}_4$  differs from the theoretical value (170  $\text{mAh}^{-1}\text{g}$ ), since the number of Li atoms per unit of  $\text{LiFePO}_4$  is 0.6 in reality.<sup>7</sup> To explain the correlation between the characteristics and microstructure of these various materials, Nuclear Magnetic Resonance (NMR) studies are needed. NMR is a valuable tool for probing the structural changes that arise in electrode materials during electrochemical battery cycling. The resonances of  $^7\text{Li}$  in diamagnetic chemical environments like in an electrolyte and the SEI (surface electrolyte interphase) are shown at about  $\pm 10$  ppm. Alternatively, the resonances of  $^7\text{Li}$  in

paramagnetic phases can be made as large as  $-500$  to  $+3000$  ppm, since the unpaired electrons from the paramagnets are capable of hyperfine interaction with them. Metallic lithium can be shifted about 250 ppm by Knight shift, which occurs when the nuclear spins interact with the unpaired electrons positioned at the Fermi level on the conduction band.<sup>8</sup> The  $^7\text{Li}$  and  $^{19}\text{F}$  solid-state NMRs are extremely useful to characterize  $\text{LiPF}_6$  which is normally used as an electrolyte as well as  $\text{LiF}$  which is a decomposed product of  $\text{LiPF}_6$ , and other lithium and fluorine compounds, or a mixture of materials in various lithium-ion batteries.  $^{19}\text{F}$  NMR experiments can possibly identify fluorine-containing compounds that are discriminable from the PVDF binder signal.<sup>8-10</sup> Correlations between the quantity of  $\text{LiF}$  on the cathode with respect to the number of cycles and the percentage of lithium loss from the cathode can be obtained. The structure in the solid electrolyte interphase was monitored quantitatively in a rechargeable LIB at both graphite and electrodes.<sup>11</sup> We designed, constructed, and tested an  $^7\text{Li}$  and  $^{19}\text{F}$  double-resonance 600-MHz solid-state NMR probe with a solenoidal coil using a Cross-Waugh circuit.<sup>12-14</sup>

### Experimental Methods

**Probe Design and Probe Construction.** The previously reported model for the design of a simple and effective probe was adapted, because the probe, which is the important interface between all NMR samples and the magnet fields resulting from RF pulses, has the strongest effects on the entire performance of the experiments.<sup>15-17</sup> All materials for the probe were prepared from nonmagnetic materials. 6061 aluminum pipe was used for the probe body with a 39.5-mm OD (outer diameter) and 39.1-mm ID (inner diameter). The probe utilized a solenoid coil, as in most solid-state NMR

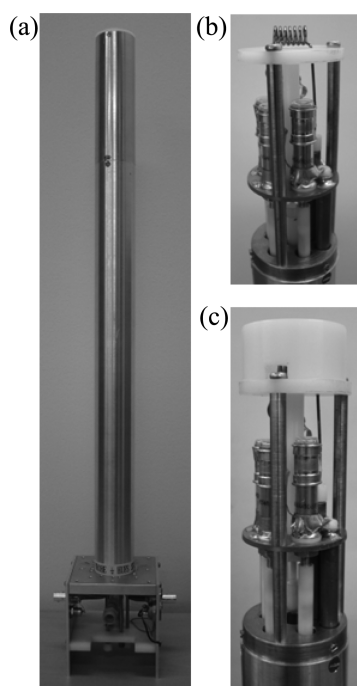


**Figure 1.** Pictures of the custom-built  $^{19}\text{F}$ - $^7\text{Li}$  double-resonance probe with solenoidal coil for a 600-MHz narrow bore magnet. (a) Overall shape of custom-built probe. (b) The probe head circuit without a cap. (c) The probe head circuit with a cap, which fully covered the solenoidal coil to minimize the heat loss. All capacitors and the probe cap are made with quartz and PE (polyethylene), respectively, to prevent fluorine signal interference from the PTFE materials used.<sup>16</sup>

probes, and the two channels ( $^7\text{Li}$  and  $^{19}\text{F}$ ) used a Cross-Waugh circuit for the double-tuned configuration.<sup>18-20</sup> The lithium ion battery for *in-situ* analysis had dimensions of 1.2 mm  $\times$  4 mm  $\times$  1 mm. A 7-turn round solenoidal coil with an ID of 5 mm and length of 15 mm was made from antique copper (Parawire, USA). To minimize the heat loss in high temperature experiments, the probe cap that fully covers the probe coil was designed using PE (polyethylene), because PTFE (polytetrafluoroethylene) contains fluorine, which would produce an interference signal with the  $\text{LiPF}_6$  lithium ion battery electrolyte and PVDF binder, as shown in Figure 1. A schematic of the finalized probe circuit is shown in Figure 2. L1 indicates 7 turns of the solenoidal coil. C1-C4 are variable quartz capacitors (NMQM10 Voltronics Corp., USA), and C5-C7 are fixed capacitors (American Technical Ceramics, US). Variable capacitors C1 and C2 were concerned by tuning and matching the lower-frequency  $^7\text{Li}$  channel ( $\nu_0 = 233$  MHz). The 2.7-pF fixed capacitor C5 was placed on the side of the solenoidal coil. The 27-pF fixed capacitor C6 and inductance L2 were used as a high-frequency trap for better isolation between the high-frequency  $^{19}\text{F}$  channel and low-frequency  $^7\text{Li}$  channel. Variable capacitors C3 and C4 were non-magnetic variable capacitors with a changeable range between 1 and 10 pF, and were used along with  $\lambda/4$  coaxial cable for tuning and matching for the high-frequency  $^{19}\text{F}$  channel operating at 564 MHz. C7 is an optional fixed capacitor in the high-frequency channel, and

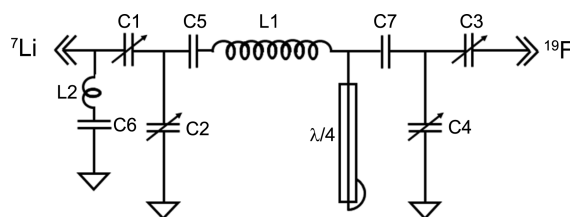


**Figure 2.** Schematic circuit diagram of  $^7\text{Li}$  and  $^{19}\text{F}$  double resonance probe with a solenoid coil for the 600-MHz narrow-bore magnet. Capacitors C1 and C2 were used for tuning and matching the lower frequency  $^7\text{Li}$  channel of 233 MHz. C3 and C4 were used for the higher frequency  $^{19}\text{F}$  channel of 564 MHz. All variable capacitors of C1 to C4 have a changeable range between 1 and 10 pF. Capacitors C5 to C7 have fixed values of 2.7 pF, 27 pF, and 3.0 pF, respectively. L1 is a 7-turn round coil with ID of 5 mm and length  $L$  of 15 mm, and the  $\lambda/4$  coaxial cable length is optimized to 8.66 cm. The probe circuit was matched to an impedance of 50  $\Omega$ .

was used to balance the sample coil, since the inductance reduces the voltage on the low side channel. C7 can be omitted unless a large  $B_1$  field is needed.<sup>18</sup> The  $\lambda/4$  coaxial line length was calculated considering the  $^{19}\text{F}$  resonance frequency at 600-MHz NMR using the following equation:

$$\begin{aligned} \text{Length of } \lambda/4 \text{ cable} &= \frac{c \cdot k}{4 \cdot \nu} \\ &= \frac{3.00 \times 10^{10} (\text{cm/sec}) \times 0.651}{4 \times 564 \times 10^6 (\text{cm/sec})} \\ &\doteq 8.66 (\text{cm}) \end{aligned}$$

$c$  indicates the speed of light,  $\nu$  is the resonance frequency of the fluorine channel with a 14.1-T magnet, and  $k$  is the shortening factor of the modified coaxial cable. The original semi-rigid coaxial cable filled with PTFE materials acted as obstacles that impede the fluorine signals, because the coaxial cable was placed close to the sample coil and connected to the coil directly. The shortening factor of the coaxial cable was changed and optimized with a previous custom-built probe.<sup>16,17</sup> Isolation between the  $^{19}\text{F}$  channel and the  $^7\text{Li}$  channel was obtained with a high-frequency trap of L2 and C6. To measure the effectiveness of LC trap with a fixed capacitor, a network analyzer (Hewlett Packard 85046A, USA) was used for monitoring the transmission between the high-frequency channel and low-frequency channel while the inductance L2 and fixed capacitor C6 were changed. The final optimized isolation value from the  $^{19}\text{F}$  channel to the  $^7\text{Li}$  channel was 46 dB, and that from the  $^7\text{Li}$  channel to the  $^{19}\text{F}$  channel was 48 dB, which are much higher values than the normal value of 25 dB. The whole probe circuit was matched to the 50- $\Omega$  value of NMR console impedance, which was matched using a network analyzer. The final tuning ranges of the high-frequency channel and low-frequency channel were 540 MHz to 582 MHz and 231 MHz to 238 MHz, respectively. An additional temperature control unit composed of a ceramic heater, a thermocouple temperature sensor, and a dewar were installed to observe the structural changes of the  $^{19}\text{F}$ -containing electrolytes and the

binder of the Li ion battery for variations of temperature.

**Solid-State NMR Experiments.** The solid-state NMR spectra were obtained using a Bruker Avance III spectrometer operating at 600 MHz for  $^1\text{H}$  with a custom-built solenoidal coil probe. We performed the experiment with TFA (trifluoroacetic acid) for  $^{19}\text{F}$  resonance and an  $\text{LiCl}_3$  liquid sample for the  $^7\text{Li}$  resonance signal. An  $\text{LiF}$  powder sample was used to confirm the chemical shift anisotropy pattern with all principal elements with  $\sigma_{11}$ ,  $\sigma_{22}$ , and  $\sigma_{33}$ . All experiments were conducted with direct polarization. A TFA and  $\text{LiCl}_3$  solution was placed in a capillary tube, sealed at both sides, and then wrapped with a polyethylene bag. The  $\text{LiF}$  powder was prepared in a solid-state NMR rotor.  $^{19}\text{F}$  and  $^7\text{Li}$  NMR spectra were observed for *in-situ* analysis of lithium ion battery made suitable for 5 mm solenoidal coil of custom-built probe. (data not shown)

### Results and Discussion

The experimental results obtained using the 600-MHz  $^{19}\text{F}$ - $^7\text{Li}$  double-resonance custom-built probe are shown Figure 3 and Figure 4. The  $^7\text{Li}$  spectrum of  $\text{LiCl}_3$  in Figure 3(a) shows one sharp and symmetrical signal without any other lithium background signals. The broad signal reflects the chemical shift anisotropy pattern of the  $\text{LiF}$  powder sample in Figure 3(b). An NMR experiment to identify the  $^7\text{Li}$  background signal from the probe was not carried out, since no lithium materials were used for probe assembly. Since broad  $^{19}\text{F}$  background signals are very well known even in commercialized probes to interfere with the analysis of the NMR spectrum, it must be removed or minimized in the  $^{19}\text{F}$

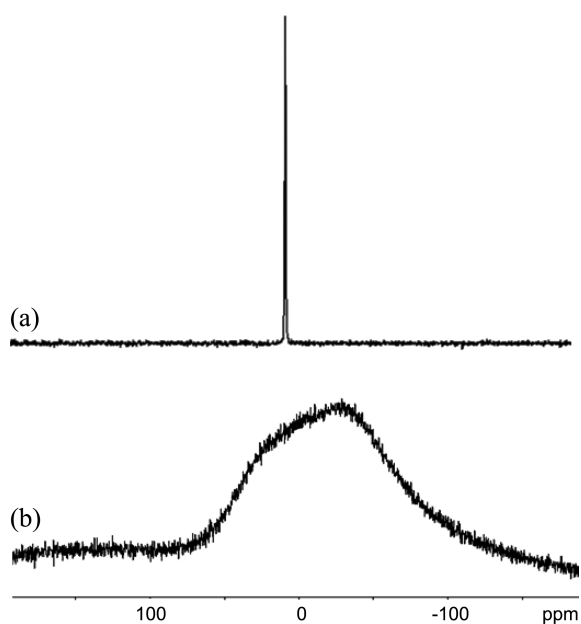


**Figure 3.** The  $^7\text{Li}$  NMR spectra of  $\text{LiCl}_3$  liquid and  $\text{LiF}$  powder samples with custom-built probe. The distinct sharp single resonance (a) indicates that the probe has a good efficiency for  $^7\text{Li}$  experiments. The broad signal (b) reflects the powder pattern of  $\text{LiF}$  powder. The  $^7\text{Li}$  background signal from the probe itself was not observed.

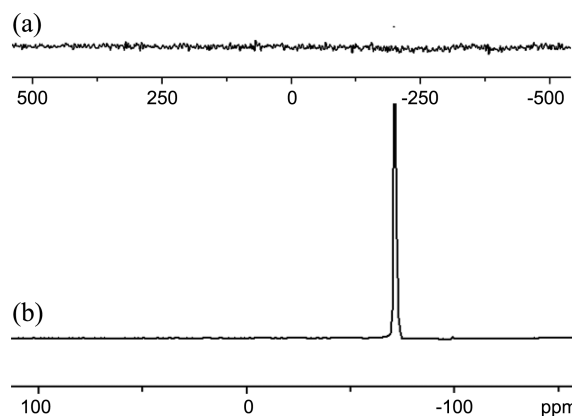


**Figure 4.** (a) An  $^{19}\text{F}$  background signal was not revealed at all over the range of  $-500$  ppm to  $500$  ppm. (b) The  $^{19}\text{F}$  resonance of trifluoroacetic acid was shown at  $-76.55$  ppm with a clear singlet, which demonstrates that there is no  $^{19}\text{F}$  background signal. The custom-built probe has good efficiency.

components of the probe circuit for the best probe efficiency. Figure 4(a) shows that no  $^{19}\text{F}$  background signal was revealed from  $-500$  ppm to  $500$  ppm. The  $^{19}\text{F}$  NMR spectrum of trifluoroacetic acid in Figure 4(b) shows a resonance at  $-76.55$  ppm with a clear singlet, which indicated that there is no  $^{19}\text{F}$  background signal. Our custom probe design and application have been demonstrated to be suitable for various  $^7\text{Li}$  and  $^{19}\text{F}$  NMR experiments.

### Conclusions

A custom-built  $^{19}\text{F}$ - $^7\text{Li}$  double-resonance solid-state NMR probe with 5-mm solenoidal coil for a 600-MHz narrow-bore magnet was successfully constructed and tested for *in-situ* studies of lithium ion batteries. The  $^{19}\text{F}$  NMR spectrum and  $^7\text{Li}$  NMR spectrum were observed for the *in-situ* analysis of lithium ion batteries. Since structural changes of the Li ion composition occur during the charge-discharge cycles of a lithium ion battery, it is essential to investigate the structural changes in a non-destructive manner in real time. Higher sensitivity and a flatter baseline than that obtained with a commercialized probe for lithium batteries were obtained (data not shown). The results have demonstrated that the proposed probe system has good efficiency and is suitable for the study of lithium ion batteries with a narrow-bore 600-MHz magnet.

**Acknowledgments.** This work was supported by the Basic Science Research Program through the National Research Foundation of Korea (NRF), funded by the Ministry of Education, Science and Technology (2010-0021954 or 2012-0007168) and the Gyeonggi Research Center Program of Gyeonggi Province (GRRC HUF5 2013-B01).

### References

- Dinh, H.-C.; Mho, S.-I.; Yeo, I.-H. *Electroanalysis* 2011, 2079, 2086.

2. Grey, C. P.; Nicolas, D. *Chem. Rev.* **2004**, 4493, 4512.
  3. Rifat, A. M.; Hikmet, R. A. M. *J. Power Sources* **2001**, 212, 220.
  4. Thackeray, M. M.; Johnson, P. J.; De Picciotto, L. A.; Bruce, P. G.; Goodenough, J. B. *Mater. Res. Bull.* **1984**, 19, 179.
  5. Ohzuku, T.; Kiagawa, M.; Hirai, T. *J. Electrochem. Soc.* **1990**, 137, 769.
  6. Tarascon, J. M.; Guyomard, D. *Electrochim. Acta.* **1993**, 38, 1221.
  7. Raver, N.; Chouinard, Y.; Magnan, J. F.; Besner, S.; Gauthier, M.; Armand, M. *J. Power Source* **2001** 503, 507.
  8. Trease, N. M.; Thomas, K.; Koster, J.; Grey, C. P. *Electrochemical Soc.* 2001.
  9. Nicolas, D.; Marine, C.; Dominique, G. *Electrochemical Soc.* **2001**.
  10. Song, S. W.; Zhuang, G. V.; Ross, P. N., Jr. *J. Electrochem. Soc.* **2004**, A1162.
  11. Meyer, B.; Leifer, N.; Sakamoto, S.; Greenbaum, S.; Grey, C. P. *Electrochem. Solid-State Lett.* **2005**, A145.
  12. Cross, V. R.; Hester, R. K.; Waugh, J. S. *Rev. Sci. Ins.* **1976**, 1486, 1488.
  13. Doty, F. D.; Inners, R. R.; Ellis, P. D. *Journal of Magnetic Resonance* **1981**, 399, 416.
  14. Jiang, Y. J.; Pugmire, R. J.; Grant, D. M. *Journal of Magnetic Resonance* **1987**, 485, 494.
  15. Wu, C. H.; Grant, C. V.; Cook, C. V.; Park, S. H.; Opella, S. J. *J. Magn. Reson.* **2009**, 74.
  16. Park, T. J.; Kim, J. S.; Um, S. H.; Kim, Y. *Bull. Korean Chem. Soc.* **2010**, 1187, 1191.
  17. Choi, S. S.; Jung, J. H.; Park, Y. G.; Park, T. J.; Park, G. H. J.; Kim, Y. *Bull. Korean Chem. Soc.* **2012**, 1577, 1580.
  18. Cross, V. R.; Hester, R. K.; Waugh, J. S. *Review of Scientific Instruments* **1976**, 1486, 1488.
  19. Doty, F. D.; Inners, R. R.; Ellis, P. D. *Journal of Magnetic Resonance* **1981**, 399, 416.
  20. Jiang, Y. J.; Pugmire, R. J.; Grant, D. M. *Journal of Magnetic Resonance* **1987**, 485, 494.
  21. Peter, L.; Eduard, G. K. Y.; Chekmenev, R. Fu.; Jun, H.; Cross, T. A.; Myriam, C.; William, W. Brey. *Journal of Magnetic Resonance* **2006**, 9, 20.
-